Stanford Exploration Project, Report 94, November 11, 1997, pages 53–61

Systematic AVO response with depth

Danielle Boyd[1]

keywords: *AVO*

ABSTRACT

Well logs reaching several kilometers into the surface of the earth show that the P-wave reflection coefficient changes behavior with depth. I examined one particular well log, reaching approximately 5 km below the surface of the earth and assumed to be saturated with water. Simple two-layer models consisting of an upper layer of saturated sand and a lower layer of shale were constructed for three different depths to study the AVO response. Studying how the amplitude variation with offset (AVO) response changes with depth for brine and gas saturated sand shows that the well log exhibits all three classes of reflectivity. The shallow portions of the well display typical Class III reflections. The deepest sections exhibit Class I behavior. Near 2.4 km, the well log comes to a crossover point and displays Class II reflection behavior.

INTRODUCTION

The reflectivity properties of layers of sand and shale are described by three classes: Class I contains those shale over sand boundaries with high positive P-wave reflection coefficients, Class II has near zero coefficients and Class III has large negative reflection coefficients (Rutherford and Williams, 1989).

Interfaces at the same CMP position, but at different depths, may show all three effects if there is a crossover in the well log data. A crossover means that if the sand layers nearest the surface have higher porosities than the adjacent shale layers, then the sand layers deepest in the well have lower porosities than the adjacent shale layers. Velocity data exhibit a similar behavior in well logs that cross over. If the P-wave velocity of the sand layers is faster than those of shale at the surface, then the deepest layers have higher P-wave velocities in the shale than in sand layers. In such a well we can study the systematic AVO response as the sand and shale layers change from Class I to Class II and finally to Class III or alternatively from Class III to Class I.

I studied the AVO response of one particular well, which was deep enough ($\approx$ 5 km)

[1]**email:** danielle@sep.stanford.edu

that crossover was likely. The aim of the project was to study the trends of AVO response for for three different saturating fluids. As the actual well was saturated by only one fluid (water), I approximated the V_p and V_s trends of the same well with the sand saturated with oil and then with with gas. These calculated values were used to model the AVO response with depth for saturation by these other fluids.

DATA

The data set used in this paper was taken from a well and was provided by Tapan Mukerji. It contained depth, travel time, volume shale fraction, porosity and density. The well extended 4.6568 km below the surface of the earth and readings of each variable were taken at every foot starting 1.1909 km below the surface.

First bad data was eliminated by removing any point where the travel time was found to be less than zero. The P-wave velocity was then found by taking the inverse of the slowness (which was measured in microseconds per foot) and converting to metric units. The S-wave velocity was necessary to compute AVO, and since S-wave velocities were not actually measured, it was calculated using the empirical methods described below.

As these empirical methods of determining S-wave velocities are simply straight lines drawn through three different sets of data relating V_p to V_s a particular rock type, the values are most likely not completely accurate for every set of data. However, the values determined for V_s by empirical relationships are useful for this project. S-wave velocities of shale layers (fraction of shale greater than 0.5) were calculated using the Mudrock line (Castagna et al., 1985).

$$V_s = .8621 V_p - 1.1724 \tag{1}$$

S-wave velocities of sand layers (fraction of shale less than 0.5) were calculated using the Han line (Han, 1986).

$$V_s = .7936 V_p - .7868 \tag{2}$$

The data set was then decimated to smooth the trends as well as make the data set smaller and easier to work with. The resulting data set was only 277 points long. The bulk moduli (K) and shear moduli (μ) were calculated based on the velocities and the following equations.

$$K = \rho(V_p^2 - \frac{4}{3}V_s^2) \tag{3}$$

$$\mu = \rho V_s^2 \tag{4}$$

Upon close examination of the data from this well log, one can see that this well does indeed match the specifications of the project. Figure 1 shows the velocities as a function of depth. From this graph, it appears as if the sand and shale velocities may cross over. Straight lines fitted to each set of velocities are shown in Figure 2. The fitted lines intercept approximately 2.4 km below the surface.

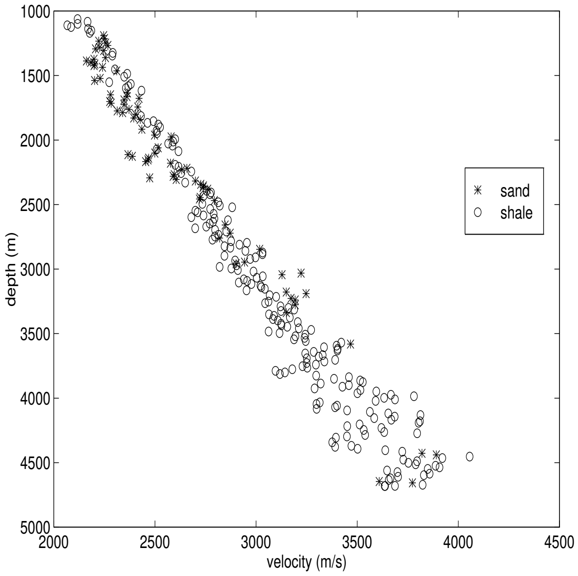

Figure 1: Velocity as a function of depth showing that it is likely that the velocities of sand and shale cross over somewhere near the center of the well. danielle-velupsidedown [NR]

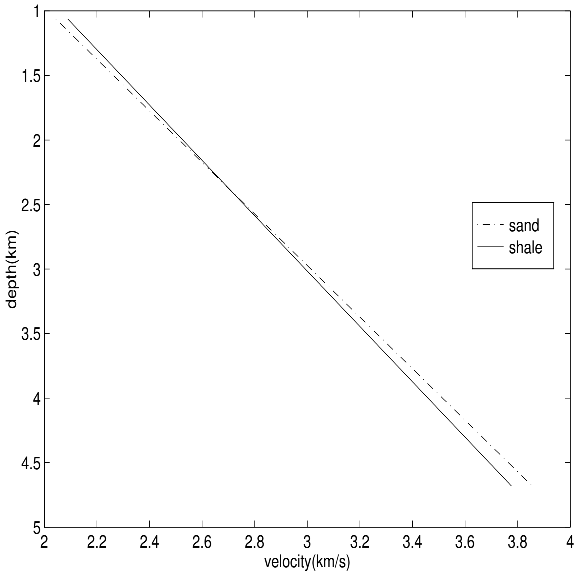

Figure 2: Fitting velocity as a function of depth shows that the sand and shale velocities do cross over. danielle-velfitupside [NR]

CLASSIFYING

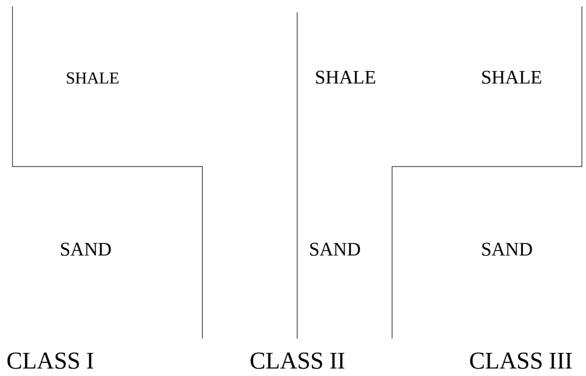

Figure 3: The three classes of reflectivity. The upper layer is a sand layer and the lower layer is a shale layer. Plotted to the right is impedance and depth is down. The shallow sections of the well exhibit Class III behavior. At 2.4 km the well exhibits Class II behavior and the deepest sections display Class I behavior. danielle-classes [NR]

The three classes of reflectivity are shown in Figure 3. The V_p, V_s and ρ (density) of shale as a function of depth were all fitted to straight lines. Subsequently, the same three properties (V_p, V_s and ρ) of sand were fitted to straight lines. I picked three different depths at which to calculate these six well properties. I then used these values to construct simplistic two-layer models. The depths used were two, 2.4 and four kilometers below the surface. The medium depth (2.4 km) was chosen specifically because it is the crossover point (V_p(sand)=V_p(shale)) and therefore, a Class II reflection. The shallow and deep depths were simply chosen to be depths significantly far from 2.4 kilometers and on opposing sides. Looking at Table 1, it is obvious that the depth closest to the surface is an example of Class III reflectivity as $V_p(shale) > V_p(sand)$. For similar reasons, the deepest portion is a class I well as $V_p(shale) < V_p(sand)$. This is obviously an example of Class II reflectivity.

AVO

An image of the AVO response of the entire data set is shown in Figure 4. It was generated by the Haskell reflectivity method. The systematic study of AVO with depth was done by fitting P-wave velocity, S-wave velocity and density to straight lines separately for sand and shale, thus establishing a trend for each of the variables. A two-layer earth model was then created by choosing several depths and picking the V_p, V_s and the density for both the shale and the sand trends. The top layer was shale and the bottom layer was sand. The sand was assumed to be saturated with water.

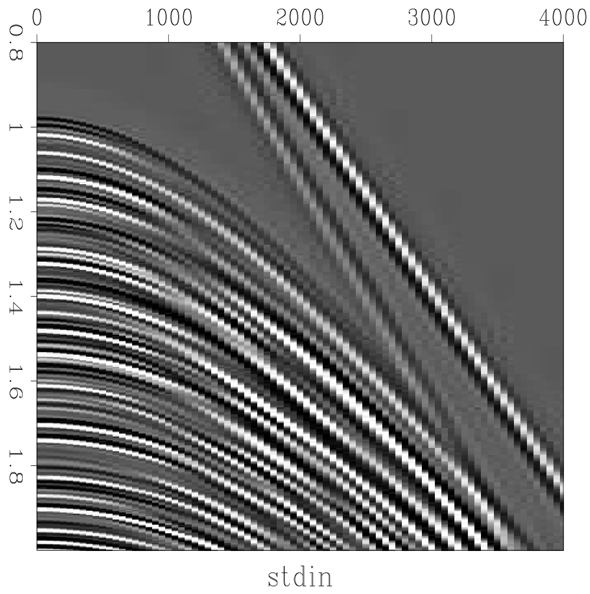

Figure 4: Synthetic seismogram generated from well log danielle-complete [ER]

FURTHER STUDY: OIL AND GAS

The next obvious step is to look at the AVO response with the sand saturated with oil and gas to see how the AVO changes with depth and with different fluids. Gassmann's Relations (Gassmann, 1951) are used to transform the data.

$$\frac{K_2}{K_{min} - K_2} - \frac{K_{fl2}}{\phi(K_{min} - K_{fl2})} = \frac{K_1}{K_{min} - K_1} - \frac{K_{fl1}}{\phi(K_{min} - K_{fl1})} \tag{5}$$

and

$$\mu_2 = \mu_1 \tag{6}$$

where K_{min} is the bulk modulus of the mineral, K_{fl} is the bulk moduli of the fluid, K_1 is the bulk modulus of the rock saturated with the original fluid (water in this case), K_2 is the bulk modulus of the rock with fluid substitution, ϕ is porosity, and μ is the shear modulus. To find the new moduli, recompute the velocities with the equations:

$$V_p = \sqrt{\frac{K_2 + \frac{4}{3}\mu_2}{\rho_2}} \tag{7}$$

$$V_s = \sqrt{\frac{\mu_2}{\rho_2}} \tag{8}$$

From the preliminary look at the AVO response, it was difficult, if not impossible, to detect any changes in the amplitude as a function of offset. The AVO of the same depths with gas and oil as the saturating fluid were almost identical to the water saturated images. This aspect of the project will, therefore, need to be studied further before any conclusive results can be stated.

RESULTS

Figure 5 shows reflection coefficient as a function of angle for a shale/sand interface at 1.5 km depth. Figures 6 and 7 show the same for interfaces at 2.4 km and 4 km depth.

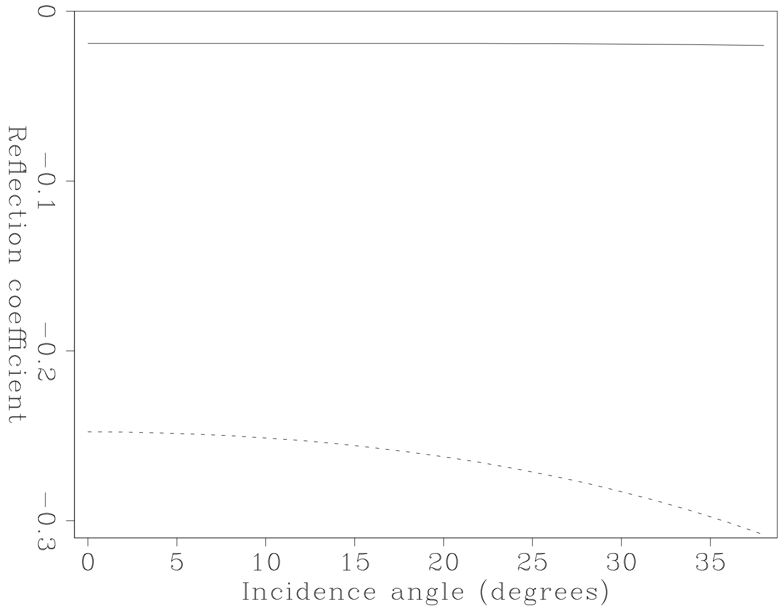

Figure 5: Reflection coefficient verses reflection angle at 1.5 kilometers. Gas saturated is plotted with a dashed line and brine saturated is plotted with a solid line. danielle-zprtz.1500 [ER]

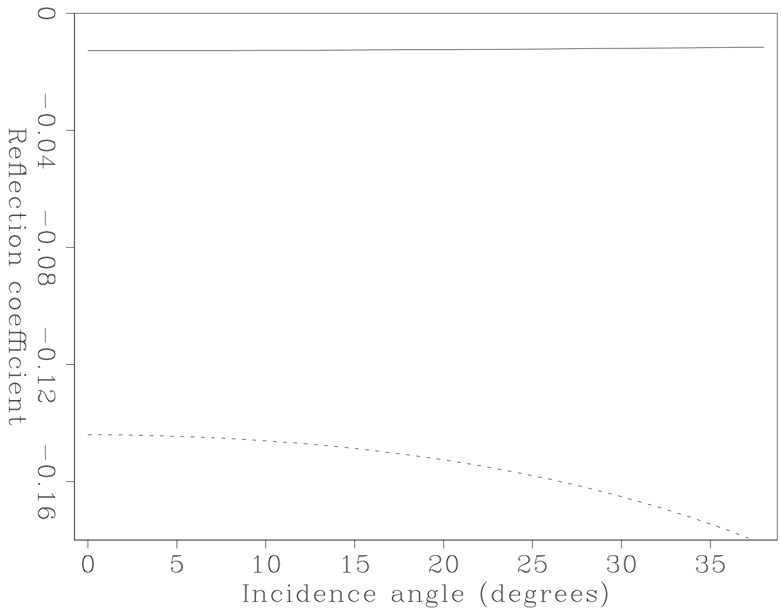

Figure 6: Reflection coefficient verses reflection angle at 2.4 kilometers. Gas saturated is plotted with a dashed line and brine saturated is plotted with a solid line. danielle-zprtz.2400 [ER]

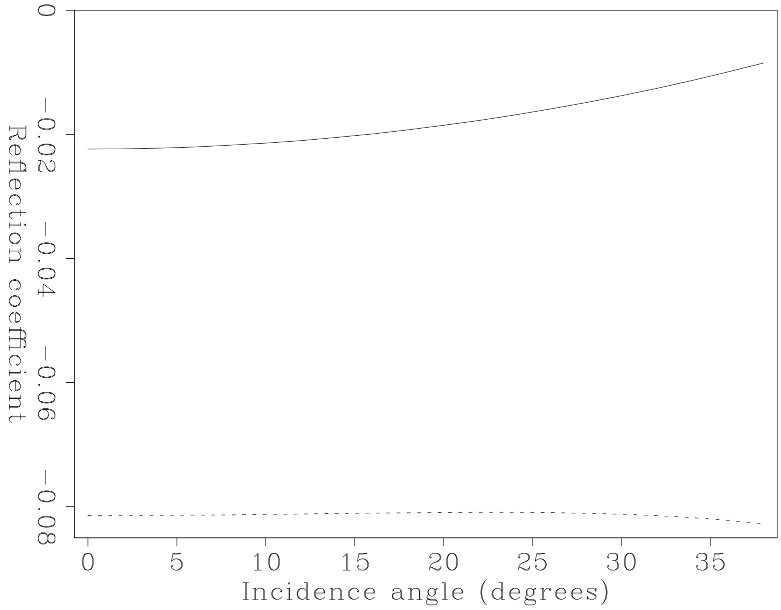

Figure 7: Reflection coefficient verses reflection angle at 4 kilometers. Gas saturated is plotted with a dashed line and brine saturated is plotted with a solid line. danielle-zprtz.4000 [ER]

CONCLUSIONS

The reflection coefficients calculated using Zoeppritz equations plotted against angle of incidence show exactly what we expected. The highest layers of the well show a typical Class III interface. This is what we would expect to find when a low impedance saturated sand layer is directly beneath a high impedance shale layer. The gas saturated shale is shown by a dashed line and the brine sand is plotted with a solid line. One can see that the AVO response of the shale over gas saturated sand increases dramatically with angle in the shallow sections of the well. The central portion of the well (approximately 2.4 km below the surface) exhibit typical Class II behavior found in areas of little impedance contrast between the shale and adjacent sand layers. Again, the brine values are plotted with a solid line and the gas saturated sands is represented with a dashed line. Finally, one can see that the deepest sections of the well behave as Class I wells should behave. The high impedance sand cause an increasing negative amplitude with angle. It is also interesting that the effect of the gas on reflection coefficient is less in the deep section of the well, due to the effect of the overburden pressure.

REFERENCES

Castagna, J. P., Batzle, M. L., and Eastwood, R. L., 1985, Relationships between compressional-wave and shear-wave velocities in clastic silicate rocks: Geophysics, **50**, no. 4, 571–581.

Gassmann, F., 1951, Uber die elastizitat poroser medien: der Natur Gesellschaft, **96**, 1–23.

Han, D.-F., 1986, Effects of porosity and clay content on acoustic properties and unconsolidated sediments: Ph.D. thesis, Stanford University.

Rutherford, S. R., and Williams, R. H., 1989, Amplitude-versus-offset variations in gas sands: Geophysics, **54**, no. 6, 680–688.